BJR

https://doi.org/10.1259/bjr.20170744

Received: 01 October 2017 | Revised: 16 January 2018 | Accepted: 23 January 2018

Cite this article as:
Bulut E, Pektas E, Sivri HS, Bilginer B, Umaroglu MM, Ozgen B. Evaluation of spinal involvement in children with mucopolysaccharidosis VI: the role of MRI. *Br J Radiol* 2018; **91**: 20170744.

FULL PAPER

Evaluation of spinal involvement in children with mucopolysaccharidosis VI: the role of MRI

[1]ELIF BULUT, MD, [2]EMINE PEKTAS, MD, [2]HATICE S SIVRI, MD, [3]BURCAK BILGINER, MD, [4]MUMTAZ M UMAROGLU, RA and [1]BURCE OZGEN, MD

[1]Department of Radiology, Hacettepe University Faculty of Medicine, Ankara, Turkey
[2]Department of Pediatric Metabolism, Hacettepe University Faculty of Medicine, Ankara, Turkey
[3]Department of Neurosurgery, Hacettepe University Faculty of Medicine, Ankara, Turkey
[4]Department of Biostatistics, Hacettepe University, Ankara, Turkey

Address correspondence to: Dr Elif Bulut
E-mail: *drelifbulut@yahoo.com*

Objective: To evaluate spinal MRI features of mucopolysaccharidosis (MPS) VI and to assess the correlation with clinical findings.
Methods: We retrospectively evaluated spinal MRI scans and clinical findings at the time of imaging in 14 patients (8 male, 6 female) with MPS VI. Craniometric measurements were performed and the images were assessed for bony anomalies, spinal stenosis and spinal cord compression. The degree of cervical cord compression was scored and correlated with neurological examination findings at the time of imaging. Vertebral alignment, structural changes in spinal ligaments and intervertebral discs were also assessed.
Results: All patients had cervical stenosis due to bony stenosis and thickened retrodental tissue (median: 6.05 mm, range 3.3–8 mm). Retrodental tissue thickness was found to increase with age (p = 0.042). Compressive myelopathy was detected at upper cervical level in 11 (79%) and lower thoracic level in 2 patients (14%). Significant inverse correlation was found between cervical myelopathy scores and neurological strength scores. The most common bony changes were hypo/dysplastic odontoid; cervical platyspondyly with anterior inferior beaking; thoracic posterior end plate depressions and lumbar posterior scalloping. Kyphosis due to retrolisthesis of the beaked lumbar vertebrae and acute sacrococcygeal angulations were other remarkable findings.
Conclusion: MRI is an essential component in evaluation of spinal involvement in MPS VI, and scanning of the entire spine is recommended to rule out thoracic cord compression.
Advances in knowledge: This study provides a detailed description of spinal MRI findings in MPS VI and underlines the role of MRI in management of cord compression.

INTRODUCTION

Mucopolysaccharidosis Type VI (MPS VI) or Maroteaux–Lamy syndrome is a rare autosomal recessive lysosomal storage disease caused by impaired catabolism of dermatan sulfate. Deficiency of the enzyme N-acetylgalactosamine 4-sulfatase, also called arylsulfatase B, leads to progressive accumulation of partially degraded dermatan sulfate within a variety of tissues with consequent clinical manifestations such as hearing impairment, organomegaly, bone dysplasia, cardiorespiratory and neurological problems.[1] Neurologic manifestations are often due to bone abnormalities resulting in spinal cord or nerve root compression, carpal tunnel syndrome, optic nerve compression, jugular foramen stenosis and communicating hydrocephalus.[2] More than 130 unique mutations of the arylsulfatase B gene constitute a spectrum of clinical manifestations with respect to age of onset, rate of progression and disease severity.[2,3] Clinical phenotypes of MPS VI can be broadly categorized as slowly progressive and rapidly progressive forms. Patients with slowly progressive disease often come to clinical attention at a later age, however, they are also at risk for severe and life-threatening complications including spinal cord compression (SCC).[4]

SCC is a well-known, disabling and life-threatening complication of MPS VI. SCC can occur at any level but craniovertebral junction (CVJ) is by far the most commonly detected region. SCC at the CVJ usually results from retrodental tissue thickening due to glycosaminoglycan accumulation, ligamentous hypertrophy and bony stenosis.[4–8] Cervical instability is a less commonly seen cause of SCC in MPS VI compared to MPS IV.[5]

Although MPS VI-related bony abnormalities of the spine were previously defined from radiographic images, MRI is necessary to appreciate structural changes in ligaments

and intervertebral discs, as well as SCC and signal abnormalities representing myelomalacia within spinal cord.[9,10] Familiarity with MRI findings is important for better understanding the natural history of spinal involvement, for evaluating effects of current and future medical treatments, for revealing risks of irreversible cord damage, and for guiding clinical management decisions such as timing for decompression surgery.

Accordingly, the aim of the present study was to describe spinal MRI findings of MPS VI in detail and to assess correlation with clinical findings especially with respect to the spinal stenosis.

METHODS AND MATERIALS

Patients

We retrospectively evaluated MRI studies of 14 MPS VI patients (8 male, 6 female) scanned between July 2009 and November 2015. Demographics and clinical data were acquired from patient charts. Inclusion criteria were biochemically confirmed diagnosis of MPS VI, availability of technically adequate spinal MRI and record of clinical data including neurological examination at the time of imaging. The neurological examination data included assessments of muscle strength, tendon reflexes and presence of pyramidal tract signs. The muscle strength of each extremity was scored using Medical Research Council scale. The previously defined strength subscale of the "Severity Score System for Progressive Myelopathy" was used to calculate the strength score of each patient by adding MRC scores of four extremities.[11]

Imaging

MRI studies were performed with a 1.5 T scanner (Siemens, Erlangen, Germany; Philips Healthcare, Best, Netherlands or GE Healthcare, Milwaukee, Wisconsin) without anaesthesia or sedation. The MRI of a patient at 2 years of age was obtained after sleep deprivation. Spinal MRI protocol included axial and sagittal planes using T_1W and T_2W pulse sequences. Parameters used in sequences were depicted in Table 1.

Image evaluation

A total number of 15 spinal and 7 brain MRI studies, including one follow-up spinal study, were assessed blindly by two neuroradiologists in consensus.

The CVJ was evaluated with respect to craniometric measurements, bony anomalies, stenosis and SCC. The craniometric measurements used in assessment of CVJ anomalies included clivus-canal angle and Welcher basal angle[12] (Figure 1a). Atlantoaxial gap between the posteroinferior aspect of the anterior arch of atlas and the nearest adjacent surface of the odontoid process was measured for the analysis of atlantoaxial instability. The morphology of odontoid process and odontoid deficiency were assessed. The odontoid deficiency measurements were made from the tip of odontoid ossification centre to the superior edge of the anterior arch of the atlas and compared with the previously published measurements of age and sex matched normal controls.[13] The elements of cervical stenosis including bony stenosis and retrodental tissue thickening were evaluated. The midline sagittal diameter of bony canal at the level of C1 was measured between the posterior cortex of odontoid process and the anterior cortex of posterior arch of atlas. The measurements were compared with previously published normal values for corresponding age and sex.[14] Thickness of retrodental tissue and narrowest anteroposterior diameter of spinal canal were measured from axial T_2W images with correlation with the sagittal images. Myelopathy scores were defined to grade compressive signal abnormalities in cervical spinal cord. Absence of signal abnormality was scored as 0, T_2 hyperintensity localized to dorsal cord (posterior column ± posterior horn) was scored as 1, and T_2 hyperintensity extending beyond dorsal cord was scored as 2.

Morphology of vertebral bodies and intervertebral discs, vertebral alignment and stenosis below CVJ were also evaluated. Cobb and sacrococcygeal angle measurements were used for the assessment of vertebral alignment.

Statistical analysis

Statistical analysis was performed using IBM SPSS 22 for windows package. Descriptive statistics were demonstrated as mean ± standard deviation or median (minimum–maximum) for quantitative variables, and categorical variables were summarized as the number of cases and (%). We used Pearson, Spearman or Eta correlation to measure strength ± direction of association between two variables. We also performed Kruskal–Wallis test

Table 1. Imaging parameters used in spinal MRI

	Sagittal *T*1W	Sagittal *T*2W	Axial *T*1W	Axial *T*2W
Sequence type	TSE	TSE	TSE	TSE
FOV, mm	340 × 340–160 × 160	340 × 340–160 × 160	220 × 150–140 × 140	200 × 150–140 × 140
Slice thickness, mm	3	3	4	4
Slice spacing, mm	3.3	3.3	4.4–5.6	4.4–5.6
TR, ms	360–557	2394–3827	360–557	2394–3827
TE, ms	7–14	86–132	7–14	86–122
Matrix size	320 × 320–512 × 512	320 × 320–512 × 512	320 × 196–400 × 400	320 × 196–400 × 400
Number of averages	2–3	2–3	2–3	2–3
FA	150	150	150	150

FA, flip Angle; FOV, field of view; TE, echo time; TR, repetition time; TSE, turbo spin echo.

Figure 1. (a–d) An example of CVJ evaluation in a 9-year-old male patient with MPS VI. Sagittal T_2WI (a) demonstrates Welcher basal angle (solid arrow) formed between the nasion-tuberculum and tuberculum-basion lines (solid lines), clivus-canal angle (notched arrow) formed between the lines drawn along the posterior aspects of clivus and axis (dashed lines). Double arrow shows sagittal diameter of bony canal at C1. Sagittal T_2WI (b) again shows spinal cord compression at CVJ due to hypo-dysplastic changes of odontoid (arrow), retrodental tissue thickening (star) and bony stenosis. The dysplastic changes of odontoid (arrow) are more appreciated in sagittal reformat CT image of the same patient (c). Please compare forementioned findings with normal sagittal T_2WI of a sex and age-matched control (d). CVJ, craniovertebral junction; MPS VI, mucopolysaccharidosis Type VI.

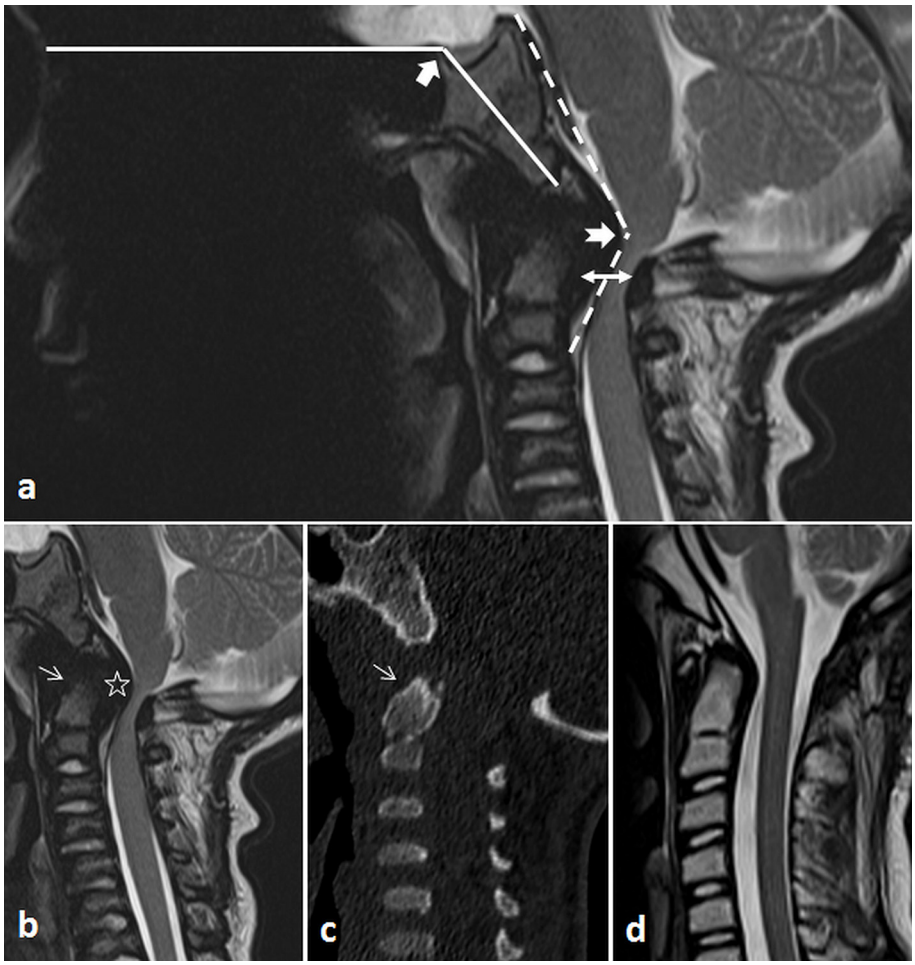

to detect if there was any difference between myelopathy scores in terms of neurological strength scores. Significant level was set at $p < 0.05$.

RESULTS

The median age of the patients at the time of MRI was 13.2 years (2.4–33 years). All patients were diagnosed with the slowly progressive clinical phenotype of MPS VI. They were already being treated [median: 37 months (2–95 months)] with enzyme replacement therapy (ERT) at the time of spinal MR scanning. The mean age at the beginning of ERT was 10.6 ± 8 years. All patients were below the 3th percentile for height.

Findings of neurological examination were summarized in Table 2. Seven patients (50%) had normal muscle strength with no signs of primary motor neuron disease, one patient had only increased tendon reflexes without muscle weakness, and six patients (43%) had paresis.

Craniovertebral junction

The clivus-canal angles [median: 141° (134–148°)] were lower than normal range (150°–180°) in seven patients (50%). Platybasia was detected in only one patient. Atlantoaxial gap was between normal ranges in all patients.

The odontoid process was hypoplastic in five patients (36%) with increased odontoid deficiency measurements [median: 5 mm (0–6.4 mm)]. Odontoid dysplasia was detected in eight patients (57%) with relatively older ages [median: 14.5 years (9–33 years)] (Figure 1b–d). Age and dysplastic changes of odontoid process showed moderate positive correlation ($r_s = 0.596$, $p = 0.025$).

All patients had thickened retrodental soft tissue [median: 6.05 mm (3.3–8 mm)]. The retrodental tissue showed low signal both in T_1W and T_2W images (Figure 1b). There was a

Table 2. The results of neurological examination, neurological assessment scores and myelopathy scales of the patients

Patient no/age (years)	MRC scale				DTR		Babinski sign R/L	Strength scale	Myelopathy scale
	RUE	LUE	RLE	LLE	RUE/LUE	RLE/LLE			
1/2	5	5	5	5	N/N	N/N	(-)/(-)	20	1
1[a] /8	2	2	3	3	↑/↑	↑/↑	(+)/(+)	10	2
2/13	5	5	5	5	N/N	N/N	(-)/(-)	20	0
3/8	5	5	5	5	N/N	N/N	(-)/(-)	20	0
4/16	5	5	5	5	N/N	N/N	(-)/(-)	20	1
5/13	3	3	3	3	↑/↑	↑/↑	(+)/(+)	12	2
6/13	5	5	5	5	N/N	N/N	(-)/(-)	20	1
7/23	5	5	5	5	N/N	N/N	(-)/(-)	20	1
8/9	2	2	2	2	↑/↑	↑/↑	(+)/(+)	8	2
9/11	5	5	5	5	N/N	N/N	(-)/(-)	20	1
10/26	3	3	3	3	↑/↑	↑/↑	(+)/(+)	12	2
11/19	4	4	4	4	N/N	N/N	(-)/(+)	16	2
12/8	5	5	5	5	↑/↑	↑/↑	(-)/(-)	20	0
13/33	4	4	4	4	↑/↑	↑/↑	(+)/(+)	16	2
14/12	4	4	4	4	↑/↑	↑/↑	(+)/(+)	16	1

[a]Follow-up evaluation.
DTR, deep tendon reflex; LLE, left lower extremity; LUE, left upper extremity; MRC, medical research council; RLE, right lower extremity; RUE, right upper extremity.

positive correlation between retrodental tissue thickness and age ($r = 0.550$, $p = 0.042$).

Sagittal diameters of bony canal at the level of C1 [median: 13.1 mm (7–17 mm)] were lower than the age and sex-matched normal ranges (−2 SD to +2 SD) (Figure 1b–d). With the accompanying thickening of retrodental tissue, the most pronounced stenosis was at the level of C1 with median canal diameter of 5 mm (3-8 mm).

Compressive cervical myelopathy with T_2 hyperintense signal change was detected in 11 patients (79%) with the age range of 2–33 years old (Figure 2 a,b and Figure 3a,b). The myelopathy scores of the patients were shown in Table 1. Age and myelopathy scores showed moderate positive correlation ($r_s = 0.547$, $p = 0.043$). The patients with normal muscle strength and no signs of primary motor neuron disease had either myelopathy score 0 ($n = 2$) or score 1 ($n = 5$). On the other hand, myelopathy scores of the patients with paresis were higher; five patients had score 2 and one patient had score 1. A statistically significant negative correlation between myelopathy scores and strength scores was found ($r_s = -0.834$). Although strength scores did not show significant difference between patients with myelopathy scores 0 and 1 ($p = 1$), they were significantly lower in patients with cervical myelopathy score 2 compared to patients with myelopathy score 0 ($p = 0.023$) and score 1 ($p = 0.015$).

Vertebral and intervertebral disc morphology

All patients had varying degrees of cervical platyspondyly. Anteroinferior beaking and posterior focal end plate depression were detected in cervical vertebrae of 11 patients (79%). These findings all together formed a vertebral shape resembling goldfish in cervical level (Figure 2c).

Although posterior focal end plate depression in thoracic vertebrae was common to all patients, anterior beaking was an uncommon finding ($n = 4$, 29%), limited to one or two vertebrae in each affected individual. Therefore, fish-shaped vertebrae at the thoracic level had rectangular heads (Figure 3c).

The morphological alterations detected in lumbar vertebral bodies were posterior scalloping ($n = 14$, 100%) and anterior beaking ($n = 9$, 64%). Posterior scalloping were also seen in lower thoracic vertebrae ($n = 6$, 43%).

Intervertebral disc morphology showed differences according to vertebral level and coexistent degeneration. Posterior focal end plate depression was associated with posterior focal thickening of corresponding discs. All patients had bulging discs at lumbar level and lumbar discs demonstrated either thickening (central or diffuse) and increased T_2 signal ($n = 7$, 50%) or height and signal loss ($n = 7$, 50%) (Figure 4). The height and signal loss of lumbar discs were more frequent in older patients ($r_{pb} = 1$).

Vertebral alignment

Scoliosis was not a prominent finding; thoracic [median Cobb angle 9° (6–19°)] and lumbar (Cobb angles of 14 and 52°) scoliosis were found in 3 (21%) and 2 (14%) patients, respectively. The cause of the lumbar scoliosis was a hemivertebra in one patient.

Figure 2. (a–c) A 19-year-old female patient with MPS VI. Sagittal T_2WI of cervical spine (a) shows compressive myelopathy due to upper cervical bony stenosis and retrodental tissue thickening (star). Axial T_2WI (b) at C2 level confirms myelopathy score 2 involving almost entire transverse section of cord (arrow). Also note the resemblance of cervical vertebra bodies to the goldfish drawing on the cropped sagittal T_2WI (c). MPS VI, mucopolysaccharidosis Type VI.

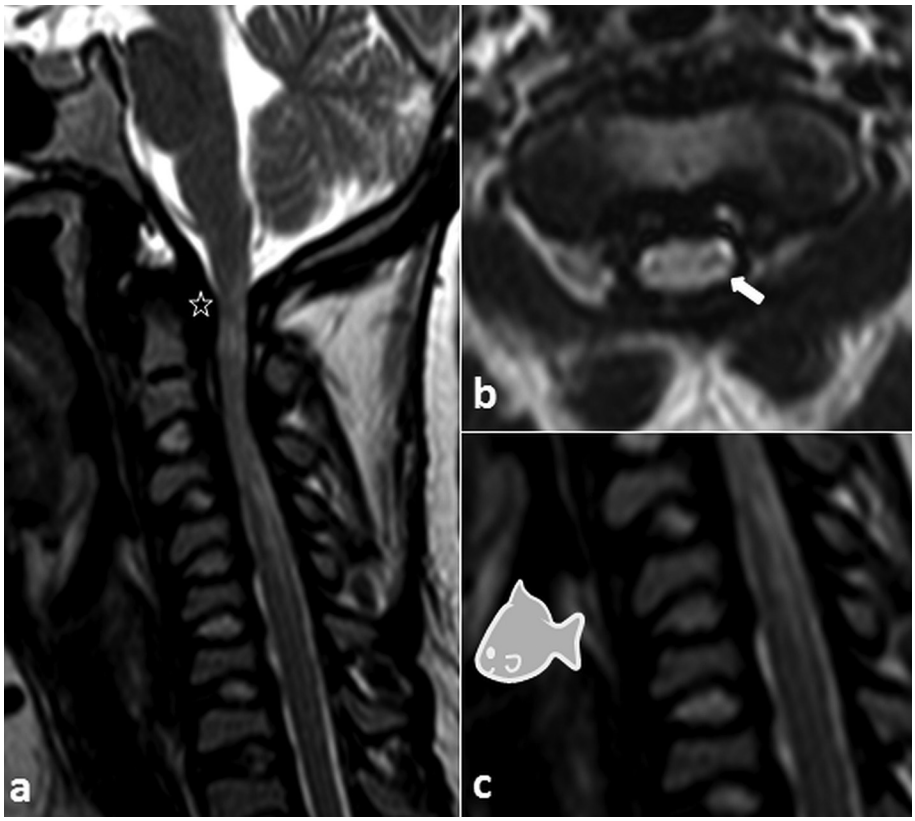

We detected thoracolumbar kyphosis in six patients (43%) with the median Cobb angle of 54.5° (19–81°), upper thoracic kyphosis in two patients with the Cobb angles of 23° and 27°. Thoracolumbar kyphosis was associated with anterior inferior beaking ± retrolisthesis of the beaked vertebra in five patients and lumbar hemivertebra in one patient. Five patients (36%) had a sharp thoracolumbar angulation (gibbus deformity) (Figure 4a).

An acute angulation at the level of S4 vertebra was detected in eight patients with the mean angle of 97° (105–72°) (Figure 4a).

Thoracolumbar spinal stenosis

Lower thoracic or thoracolumbar stenosis were detected in nine patients (64%) due to bony stenosis with accompanying bulging discs ($n = 5$), thoracolumbar gibbus deformity ($n = 3$), or disc-osteophyte complexes ($n = 1$). Compressive T_2 hyperintense signal change in distal cord associated stenosis in two patients (Figure 4b). One of the patients with myelopathy revealed no neurological deficits. The other patient (no: 11) who also had compressive cervical myelopathy showed tetraparesis with left-sided Babinski sign.

Brain MRI findings

The brain MRI findings were as follows; minimal cerebral volume loss ($n = 7$, 100%), J-shaped sella ($n = 6$, 86%), minimal to moderate hydrocephalus ($n = 4$, 57%), T_2 hyperintense cerebral white matter lesions ($n = 4$, 57%), dilated perivascular spaces ($n = 3$, 43%).

Follow up

Only one patient had control spinal MRI which was performed 6 years after the first radiological evaluation. The patient was started on ERT at the age of 2 years, just 2 months before the first MRI. Follow-up MRI showed increase in retrodental tissue thickness, cervical stenosis and extend of cervical myelopathic signal change under ERT. The strength score at the time of follow-up imaging was accordingly lower with development of tetraparesis and pyramidal signs. MRI also revealed progression of thoracolumbar kyphosis with L2 retrolisthesis and degenerative changes at lumbar intervertebral discs.

Four patients who had severe neurologic deficits with neurologic assessment scores of ≤12 and myelopathy scores 2 were performed spinal decompression surgery. All patients showed significant neurologic improvement after surgery.

DISCUSSION

MRI plays a major role in evaluation of spinal involvement in MPS VI. Information on spinal MRI findings of MPS VI is limited to a few case reports and multicenter studies in literature, mainly focussing on assessment and management of cervical cord compression.[5,6,8,15,16] A study on MRI findings of the entire

Figure 3. (a–c) A 13-year-old male patient with MPS VI. Sagittal (a) and axial (b) T_2WI of cervical spine shows compressive myelopathy at CVJ due to bony stenosis and retrodental tissue thickening (star). Cervical myelopathy (arrow) is confined to dorsum of spinal cord, so graded as score 1. Also, note odontoid hypodysplasia, cervical platyspondyly and the shape of thoracic vertebrae. The fish-shaped vertebrae at the thoracic level had rectangular heads (c). CVJ, craniovertebral junction; MPS VI, mucopolysaccharidosis Type VI.

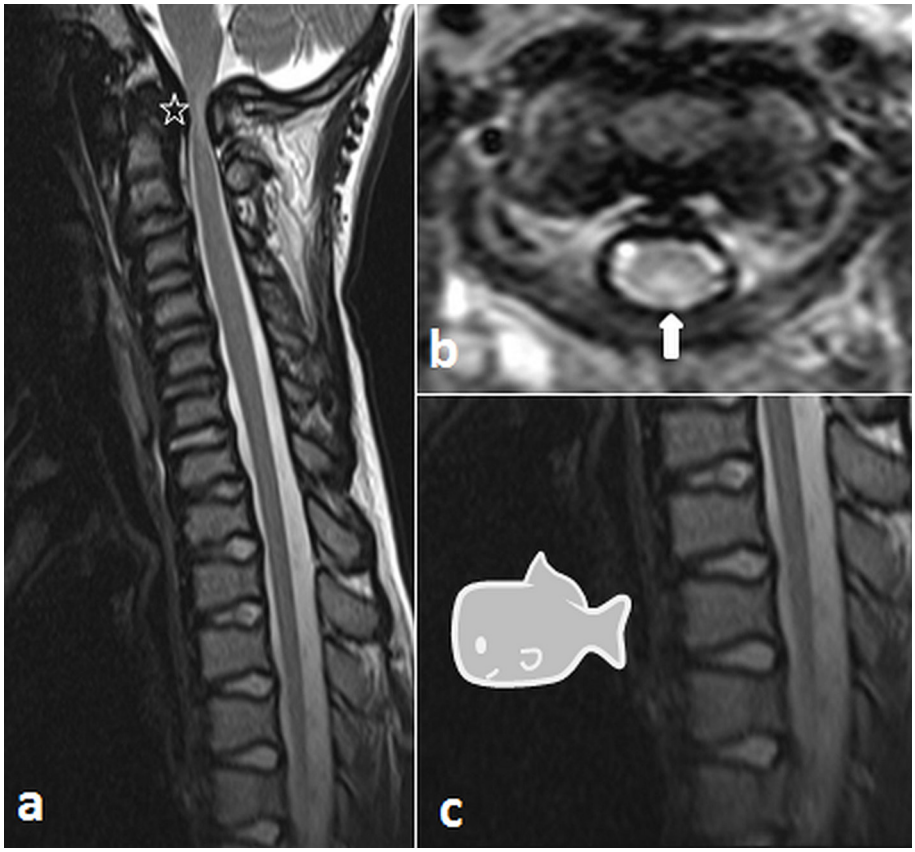

spine in a large group of MPS VI patients has not been previously reported to our knowledge. Our single centre study aims to provide a detailed description of spinal MRI findings in MPSVI and to assess correlation between imaging and neurological findings.

CVJ anomalies were common in our study. Clivus-canal angle was lower than normal range in half of the patients, probably due to odontoid dysplasia and thickened retrodental tissue. Almost all patients (93%) had hypo/dysplastic changes of odontoid. Odontoid dysplasia was more frequent than hypoplasia in older patients, which may reflect the outcome of abnormal ossification due to glycosaminoglycan accumulation.

Atlantoaxial instability is an uncommon feature in MPS VI compared to MPS IV.[5,8] It is best evaluated with dynamic flexion and extension studies of cervical spine. Dynamic MRI can also give valuable information regarding this aspect, however, it should be performed carefully under anaesthesia or sedation to avoid spinal cord injury in MPS VI patients.[8] Dynamic MRI was not performed in our study group; therefore, we used atlantoaxial gap measurement to predict cervical instability. Atlantoaxial gap was between normal ranges in all patients.

Spinal stenosis and compression were reported to be more frequent and prominent in patients with MPS IV and VI compared to patients with MPS I.[7,17] SCC may occur at any level but usually involves CVJ. Bony stenosis due to small and thickened posterior elements, thickened retrodental tissue, and odontoid dysplasia are commonly recognized causes of cervical cord compression in MPS VI.[3–5,8,15,16] Thickening of the retrodental tissue is secondary to hypertrophy of the cruciate and posterior longitudinal ligaments as well as dural accumulation of glycosaminoglycans, similar to that seen in more common type MPS 1 (3, 8, 15). All of our patients had bony stenosis at the level of C1 and thickened retrodental tissue. Thickness of retrodental tissue and age showed positive correlation which is thought to represent progressive accumulation of glycosaminoglycans during the course of the disease.

Early detection and treatment of cord compression are crucial to preclude irreversible neurologic impairment. Lampe et al developed a scoring system using findings of neurological examination, somatosensory-evoked potentials of median nerve and MRI of craniocervical junction to establish objective criteria for decision of cervical decompression surgery in MPS VI.[4] The sum of the scores of each procedure, so-called craniocervical cord

Figure 4. (a) A 13-year-old male patient with MPS VI. Sagittal T_2WI shows typical thoracolumbar gibbus formation with anterior wedging and retrolisthesis of L1 vertebra (notched arrow). Also, note posterior scalloping at thoracolumbar vertebrae (thin arrow), increased signal intensity and thickness of lumbar intervertebral discs below the level of L2 vertebra and acute sacrococcygeal angulation at S4 vertebra (circle). (b) A 13-year-old female patient with MPS VI. Sagittal T_2WI shows lower thoracic spinal stenosis and compressive myelopathy (thick arrow) due to bony stenosis and associated bulging discs. Intervertebral discs also demonstrate degenerative signal and height loss. MPS VI, mucopolysaccharidosis Type VI.

compression score, was revealed to be a reliable tool for determining need and correct timing of surgery. They also found significant relationship between findings of MRI and neurological examination. The rate of compressive T_2 hyperintense signal change at CVJ was significantly higher in our study (n = 11, 79%) compared to the study of Lampe et al (33%) in which myelopathic changes were not graded. Additionally, during image evaluation, we noticed that myelopathic changes seen in some patients were mostly confined to the dorsal cord contrary to more extensive involvement in others. Therefore, in order to assess correlation with the neurologic findings appropriately, a different scoring system which additionally grades the extent of signal change at CVJ was developed. Six patients (43%) had myelopathic signal change confined to dorsal cord (score 1), five patients (36%) had signal change extending beyond the dorsum and involving almost whole transverse section of the cord (score 2). This finding led us to suggest that myelopathic signal changes might start at the dorsum of the cervical cord in MPS VI. The extent of the signal changes was found to increase with age, which probably reflects increase in retrodental tissue thickness.

It has been reported that neurological examination may underestimate the degree of SCC revealed by MRI.[7,9,18] Similarly, the majority of our patients (83%) with myelopathy score 1 had no recorded neurological impairment. The cervical signal changes correlated well with the neurological strength scores (r_s = −0.834) and the patients with myelopathy score 2 had significantly lower strength scores compared to patients with myelopathy score 0 and 1. There was no significant difference between myelopathy score 0 and 1 in terms of strength scores. Perhaps, the dorsal cord changes that myelopathy score 1 suggests could be revealed by sensorimotor evoke potentials which evaluate the functioning of posterior columns. Therefore, myelopathic signal changes confined to dorsal cord (score 1) with associated sensorimotor evoke potentials abnormalities could be used as an early predictor of cord damage and a decision-making tool for decompression surgery. Nevertheless, these suggestions need to be validated in future studies with higher number of patients.

Morphological changes of vertebral bodies with their relative frequencies at each spinal level were evaluated in detail. Platyspondyly and anteroinferior beaking of cervical vertebrae, posterior focal end plate depression in thoracic vertebrae, posterior scalloping and anterior beaking of lumbar vertebrae were the most predominant findings. Morphologic changes of discovertebral unite (platyspondyly, focal end plate depression) likely represent the effects of glycosaminoglycan accumulation in the superior and inferior cartilaginous plates which the growth of vertebral body mostly depend on. The morphological differences between the different spinal levels might be explained by load-bearing differences at each level.

All of the patients had lumbar intervertebral disc bulging. The thickness and signal of lumbar intervertebral discs were correlated with age. The patients with relatively younger ages had thickened discs with high signal intensity probably due to glycosaminoglycan accumulation, whereas the patients with older ages had signal and height loss likely due to degeneration.

Thoracolumbar gibbus formation with or without stenosis was not infrequent (36%) and formed mostly due to retrolisthesis of wedge-shaped L1 or L2 vertebra. The anterior vertebral hypoplasia, low bone mineral density, ligamentous laxity and chronic hypotonia are thought to be responsible for thoracolumbar gibbus in patients with MPS.[19,20] The wedge formation is more frequent and prominent at first two lumbar vertebrae because these transitional zone vertebrae are more prone to flexion induced compressive spinal load.

Thoracolumbar stenosis due to bony stenosis, gibbus formation and/or bulging disc-osteophyte complexes was a common finding in our patients (64%). It was associated with compressive myelopathic signal change in two patients (14%). This finding underlines the importance of scanning the entire spine for a proper evaluation; because thoracolumbar stenosis and

associated compression findings could be masked by the findings of cervical stenosis and may be overlooked in neurologic examination.

Sacrococcygeal acute angulation at the level of dysplastic and angulated S4 vertebra was another frequent finding in our study. This finding was not defined in previous studies as far as we know. The more ventrally curved coccyx was reported to be associated with coccydynia.[21] Data regarding the symptom of coccydynia was missing in our patients, but it could be questioned in a prospective study.

Communicating hydrocephalus is common in MPS VI. It may be explained by impaired function of arachnoid granulations due to GAG accumulation or decreased cerebral venous outflow due to craniocervical dysplasia.[7] Although number of brain MRIs were limited in our study, the rate of hydrocephalus (57%) was similar to the previous report of Azevedo et al.[22]

The management of MPS VI was limited to supportive therapy and/or haematopoietic stem cell transplantation before the advent of ERT with recombinant human arylsulfatase B. ERT is recently available treatment option which attempt to change the progressive nature of MPS VI.[3,23] Statistically significant improvements in a 12-min walk test, in a 3-min stair climb, increase in height and growth rate have been demonstrated in patients receiving ERT.[3,6] Although ERT has been shown to have no influence on preventing cervical cord compression in small series,[5] studies with large number of patients should be conducted with baseline and regular follow-up evaluation to demonstrate possible spinal effects.

Our study has some limitations due to its retrospective design. First of all, only patients with slowly progressive MPS VI were evaluated. All patients were already receiving ERT at the time of imaging, so we could not evaluate pre-treatment findings. Also, we had only one follow-up study with a long interval, so we could not properly reveal the effects of ERT on spinal MRI findings. On the other hand, positive correlation of age and retrodental tissue thickness in our study and progression of MRI findings in the follow-up imaging presumably represents ongoing glycosaminoglycan accumulation in spite of ERT. The other limitations were the lack of advanced imaging such as diffusion-weighted imaging and diffusion tensor imaging for functional assessment of cord, and lack of dynamic studies for proper assessment of atlantoaxial instability. These limitations could be overcome by a prospective study designed with regular clinical and radiological examinations including diffusion-weighted imaging, diffusion tensor imaging and dynamic studies.

In conclusion, spinal MRI is very efficient in revealing spinal involvement of MPS VI, especially in terms of retrodental tissue thickening, intervertebral disc changes and SCC. The myelopathic signal changes are considered to precede neurological examination findings in cervical cord compression, which makes spinal MRI an essential component in early detection of cord compression. Spinal stenosis with consequent spinal cord and nerve root compression can also be detected in thoracolumbar level, therefore scanning of whole spine is recommended for a proper evaluation.

The study was approved by the local institutional review board (GO 14/610–09).

REFERENCES

1. Neufeld EF, Muenzer J. The mucopolysaccharidosis VI. In: Scriver CR, Beaudet AL, Sly WS, Valle D, eds. *The metabolic and molecular basis of inherited disease*. 8th ed. New York: McGraw-Hill; 2001. pp. 3421–52.
2. Valayannopoulos V, Nicely H, Harmatz P, Turbeville S. Mucopolysaccharidosis VI. *Orphanet J Rare Dis* 2010; **5**: 5. doi: https://doi.org/10.1186/1750-1172-5-5
3. Solanki GA, Alden TD, Burton BK, Giugliani R, Horovitz DD, Jones SA, et al. A multinational, multidisciplinary consensus for the diagnosis and management of spinal cord compression among patients with mucopolysaccharidosis VI. *Mol Genet Metab* 2012; **107**: 15–24. doi: https://doi.org/10.1016/j.ymgme.2012.07.018
4. Lampe C, Lampe C, Schwarz M, Müller-Forell W, Harmatz P, Mengel E. Craniocervical decompression in patients with mucopolysaccharidosis VI: development of a scoring system to determine indication and outcome of surgery. *J Inherit Metab Dis* 2013; **36**: 1005–13. doi: https://doi.org/10.1007/s10545-013-9591-5
5. Horovitz DD, Magalhães TS, Pena e Costa A, Carelli LE, Souza e Silva D, de Linhares e Riello AP, et al. Spinal cord compression in young children with type VI mucopolysaccharidosis. *Mol Genet Metab* 2011; **104**: 295–300. doi: https://doi.org/10.1016/j.ymgme.2011.07.019
6. Jurecka A, Opoka-Winiarska V, Jurkiewicz E, Marucha J, Tylki-Szymańska A. Spinal cord compression in maroteaux-lamy syndrome: case report and review of the literature with effects of enzyme replacement therapy. *Pediatr Neurosurg* 2012; **48**: 191–8. doi: https://doi.org/10.1159/000345635
7. Reichert R, Campos LG, Vairo F, de Souza CF, Pérez JA, Duarte JÁ, et al. Neuroimaging findings in patients with mucopolysaccharidosis: what you really need to know. *Radiographics* 2016; **36**: 1448–62. doi: https://doi.org/10.1148/rg.2016150168
8. Solanki GA, Sun PP, Martin KW, Hendriksz CJ, Lampe C, Guffon N, et al. Cervical cord compression in mucopolysaccharidosis VI (MPS VI): findings from the MPS VI clinical surveillance program (CSP). *Mol Genet Metab* 2016; **118**: 310–8. doi: https://doi.org/10.1016/j.ymgme.2016.06.001
9. Rasalkar DD, Chu WC, Hui J, Chu CM, Paunipagar BK, Li CK. Pictorial review of mucopolysaccharidosis with emphasis on MRI features of brain and spine. *Br J Radiol* 2011; **84**: 469–77. doi: https://doi.org/10.1259/bjr/59197814
10. Morishita K, Petty RE. Musculoskeletal manifestations of mucopolysaccharidoses. *Rheumatology* 2011; **50**(Suppl 5): v19–v25. doi: https://doi.org/10.1093/rheumatology/ker397
11. Castilhos RM, Blank D, Netto CB, Souza CF, Fernandes LN, Schwartz IV, et al. Severity score system for progressive myelopathy:

development and validation of a new clinical scale. *Braz J Med Biol Res* 2012; **45**: 565–72. doi: https://doi.org/10.1590/S0100-879X2012007500072

12. Smoker WR. Craniovertebral junction: normal anatomy, craniometry, and congenital anomalies. *Radiographics* 1994; **14**: 255–77. doi: https://doi.org/10.1148/radiographics.14.2.8190952
13. Elliott S, Morton RE, Whitelaw RA. Atlantoaxial instability and abnormalities of the odontoid in down's syndrome. *Arch Dis Child* 1988; **63**: 1484–9. doi: https://doi.org/10.1136/adc.63.12.1484
14. Pettersson H, Ringertz H. *Measurements in pediatric radiology*; 1991. pp. 22–3.
15. Mut M, Cila A, Varli K, Akalan N. Multilevel myelopathy in maroteaux-lamy syndrome and review of the literature. *Clin Neurol Neurosurg* 2005; **107**: 230–5. doi: https://doi.org/10.1016/j.clineuro.2004.05.003
16. Vougioukas VI, Berlis A, Kopp MV, Korinthenberg R, Spreer J, van Velthoven V. Neurosurgical interventions in children with maroteaux-lamy syndrome. Case report and review of the literature. *Pediatr Neurosurg* 2001; **35**: 35–8. doi: https://doi.org/10.1159/000050383
17. Zafeiriou DI, Batzios SP. Brain and spinal MR imaging findings in mucopolysaccharidoses: a review. *AJNR Am J Neuroradiol* 2013; **34**: 5–13. doi: https://doi.org/10.3174/ajnr.A2832
18. Faerber EN, Poussaint TY. Magnetic resonance of metabolic and degenerative diseases in children. *Top Magn Reson Imaging* 2002; **13**: 3–22. doi: https://doi.org/10.1097/00002142-200202000-00002
19. Garrido E, Tomé-Bermejo F, Adams CI. Combined spinal arthrodesis with instrumentation for the management of progressive thoracolumbar kyphosis in children with mucopolysaccharidosis. *Eur Spine J* 2014; **23**: 2751–7. doi: https://doi.org/10.1007/s00586-014-3186-1
20. Smith LJ, Baldo G, Wu S, Liu Y, Whyte MP, Giugliani R, et al. Pathogenesis of lumbar spine disease in mucopolysaccharidosis VII. *Mol Genet Metab* 2012; **107**: 153–60. doi: https://doi.org/10.1016/j.ymgme.2012.03.014
21. Woon JT, Maigne JY, Perumal V, Stringer MD. Magnetic resonance imaging morphology and morphometry of the coccyx in coccydynia. *Spine* 2013; **38**: E1437–E1445. doi: https://doi.org/10.1097/BRS.0b013e3182a45e07
22. Azevedo AC, Artigalás O, Vedolin L, Komlós M, Pires A, Giugliani R, et al. Brain magnetic resonance imaging findings in patients with mucopolysaccharidosis VI. *J Inherit Metab Dis* 2013; **36**: 357–62. doi: https://doi.org/10.1007/s10545-012-9559-x
23. Borlot F, Arantes PR, Quaio CR, Franco JF, Lourenço CM, Bertola DR, et al. New insights in mucopolysaccharidosis type VI: neurological perspective. *Brain Dev* 2014; **36**: 585–92. doi: https://doi.org/10.1016/j.braindev.2013.07.016